C. R. Mecanique 345 (2017) 117–124

Contents lists available at ScienceDirect

Comptes Rendus Mecanique

www.sciencedirect.com

Invariant solutions in a channel flow using a minimal restricted nonlinear model

Frédéric Alizard [a,b,*]

[a] LMFA, CNRS, Ecole Centrale de Lyon, Université Lyon 1, INSA Lyon, France
[b] DynFluid–CNAM, 151, boulevard de l'Hôpital, 75013 Paris, France

ARTICLE INFO

Article history:
Received 5 September 2016
Accepted after revision 28 November 2016
Available online 12 December 2016

Keywords:
Channel flow
Invariant solutions
Subcritical transition

ABSTRACT

Simulations using a Restricted Nonlinear (RNL) system, where mean flow distortion resulting from Reynolds stress feedback regenerates rolls, is applied in a channel flow under subcritical conditions. This quasi-linear restriction of the dynamics is used to study invariant solutions located in the bulk of the flow found recently by Rawat et al. (2016) [14]. It is shown that the RNL system truncated to a single streamwise mode for the perturbation supports invariant solutions that are found to bifurcate from a relative periodic orbit into a travelling wave solution when the spanwise size is increasing. In particular, the travelling wave solution exhibits a spanwise localized structure that remains unchanged for large values of the spanwise extent as the invariant solution lying on the lower branch found by Rawat et al. (2016) [14]. In addition, travelling wave solutions provided by this minimal RNL system are self-similar with respect to the Reynolds number based on the centreline velocity, and the half-channel height varying from 2000 to 5000.

1. Introduction

The investigation of relative invariant solutions for wall-bounded flows with homogeneous spatial directions, such as pipes and channels, helped to achieve a considerable step forward in the understanding of phase space trajectories leading to turbulence, under subcritical conditions.

In particular, travelling waves and/or relative periodic orbits have been found at Reynolds numbers much lower than the one corresponding to the onset of an exponential mode (see for instance Duguet et al. [1], Kerswell and Tutty [2], Waleffe [3] and Schneider et al. [4] for pipe, channel and Couette flows, respectively). In addition, the linearized dynamics about these solutions are found to be unstable for most of them.

In that context, several efforts have been made to show that coherent structures observed in wall turbulence result from close passes to unstable invariant solutions [5]. For instance, travelling wave solutions of channel flow concentrated near walls were numerically studied by Jimenéz and Simens [6], Gibson and Brand [7]. Previous authors suggested that these travelling waves correspond to elemental version of near-wall coherent structures. In particular, they bear strong similarities

* Correspondence to: LMFA UMR5509, 36, avenue Guy-de-Collongue, 69130 Écully, France.
E-mail address: frederic.alizard@lecnam.net.

http://dx.doi.org/10.1016/j.crme.2016.11.005

with simplified flow motions obtained by direct numerical simulations (DNS) using a "minimal" system (i.e. the smallest computational box in which turbulence may be sustained) [8,9]. A relative periodic orbit solution obtained in a minimal channel flow unit is also suggested by Toh and Itano [10] as the fundamental process of near-wall turbulence.

These solutions feature a sinuously bent low-speed streak flanked by a pair of quasi-streamwise vortices that are organized into a self-sustained cycle (see Waleffe and Kim [11]; and Duriez et al. [12] for experimental evidence). Recently, Rawat et al. [13] and Rawat et al. [14] computed invariant solutions in channel flows at Reynolds numbers based on the centreline velocity and the half channel height varying from 2000 to 5000. While invariant solutions described above are concentrated near the walls, the latter occupy the bulk of the flow. These solutions consist also in sinuous streamwise streaks, periodically or continuously forced by quasi-streamwise vortices in a self-sustained process. Rawat et al. [14] have shown that two branches of travelling wave solutions bifurcate from a relative periodic orbit when the spanwise extent is increased. While the lower branch of travelling wave solutions is characterized by a spanwise-localized pattern, structures lying on the upper branch develop multiple streaks when the spanwise size is increased. These solutions are seen to persist in the turbulent regime, giving some evidence that they are linked to self-sustained large-scale coherent motions populating the outer region [15].

Therefore, the important role of these invariant solutions in bypass transition and low-Reynolds-number turbulence requires the development of numerical methods and models aiming to overcome their expensive computational cost. For that purpose, Thomas et al. [16] and Farrell et al. [17] have recently developed a low-order model, referenced as the Restricted Nonlinear model (RNL), which involves key elements of the self-sustained process. In particular, the RNL model relies on a coupled system of equations reproducing the amplification of the streak secondary instability whose quadratic interactions regenerate rolls that induce streaks by lift-up effect and close the loop of the self-sustained process. Furthermore, Thomas et al. [16] show a close correspondence between RNL models and DNS for the case of a turbulent plane Couette flow at low-Reynolds number. In addition, the RNL system is seen to sustain a turbulent state with a small number of streamwise modes.

Hence, the goal of this work is to further investigate RNL models in reproducing invariant solutions found recently by Rawat et al. [14]. Such an analysis may thus provide a promising tool to analyze the emergence of large-scale motions in wall-bounded turbulent flows with relatively low degrees of freedom. This paper is organized as follows. Section 2 contains a derivation of the minimal RNL model where only one streamwise varying mode is considered. Section 3 is devoted to reproduce invariant solutions found by Rawat et al. [14] using the minimal RNL model. We will explore the evolution of these invariant solutions when the Reynolds number is varying from 2000 to 5000 for a wide range of spanwise sizes. Finally, a discussion follows in section 4.

2. Governing equations and numerical methods

In this section, we describe briefly the system of equations that is used. The latter is based on the previous work of Waleffe and Kim [11] and has also been recently considered by Thomas et al. [16] in the study of the self-sustaining process that maintains turbulence in Couette flow. Accounting that roll/streak dynamics is a key element of invariant solutions in wall-bounded flows, we will consider hereafter a model reproducing the so-called self-sustained process, which states that streaks are generated by the superposition of streamwise rolls and a shear flow (through the lift-up effect), being in turn sustained by the continual reformation of the roll resulting from nonlinear interactions of the streak instability mode.

Following Farrell et al. [17], we consider a plane channel flow where a constant mass flux is maintained through a time-varying pressure gradient referenced as $G(t)$. The streamwise, wall-normal and spanwise coordinates are x, y, and z, respectively. The lengths of the channel in x, y and z are L_x, $2h$ (where h is the half-channel height) and L_z, respectively. We introduce a streamwise average operator: $[\bullet]$. The instantaneous velocity field, $\mathbf{u} = (u, v, w)^{\mathrm{t}}$ (where u, v and w are the streamwise, wall normal and spanwise velocity components, respectively) is decomposed into its streamwise mean value ($\mathbf{U} = (U, V, W)^{\mathrm{t}} = [\mathbf{u}]$) and a perturbation, $\mathbf{u}' = (u', v', w')^{\mathrm{t}}$, such as $\mathbf{u} = \mathbf{U} + \mathbf{u}'$. The pressure is similarly written as: $p = -G(t)x + P + p'$. The Navier–Stokes equations for an incompressible flow are then rewritten into a coupled system for the streamwise mean velocity field and the perturbation. The set of equations for the streamwise mean velocities is given below:

$$\frac{\partial U}{\partial t} + V\frac{\partial U}{\partial y} + W\frac{\partial U}{\partial z} = G(x) + \nu\left(\frac{\partial^2 U}{\partial y^2} + \frac{\partial^2 U}{\partial z^2}\right) - \frac{\partial [uv]}{\partial y} - \frac{\partial [uw]}{\partial z} \tag{1a}$$

$$\frac{\partial V}{\partial t} = -\frac{\partial P}{\partial y} + \nu\left(\frac{\partial^2 V}{\partial y^2} + \frac{\partial^2 V}{\partial z^2}\right) - \frac{\partial [vv]}{\partial y} - \frac{\partial [vw]}{\partial z} \tag{1b}$$

$$\frac{\partial W}{\partial t} = -\frac{\partial P}{\partial z} + \nu\left(\frac{\partial^2 W}{\partial y^2} + \frac{\partial^2 W}{\partial z^2}\right) - \frac{\partial [wv]}{\partial y} - \frac{\partial [ww]}{\partial z} \tag{1c}$$

$$\frac{\partial V}{\partial y} + \frac{\partial W}{\partial z} = 0, \tag{1d}$$

with ν is the kinematic viscosity. The roll/roll interactions are assumed to be high-order terms [11] and are neglected in equations (1). The perturbation field is governed by:

$$\frac{\partial u}{\partial t}+U\frac{\partial u}{\partial x}+v\frac{\partial U}{\partial y}=-\frac{\partial p}{\partial x}+\nu\left(\frac{\partial^2 u}{\partial x^2}+\frac{\partial^2 u}{\partial y^2}+\frac{\partial^2 u}{\partial z^2}\right) \tag{2a}$$

$$\frac{\partial v}{\partial t}+U\frac{\partial v}{\partial x}=-\frac{\partial p}{\partial y}+\nu\left(\frac{\partial^2 v}{\partial x^2}+\frac{\partial^2 v}{\partial y^2}+\frac{\partial^2 v}{\partial z^2}\right) \tag{2b}$$

$$\frac{\partial w}{\partial t}+U\frac{\partial w}{\partial x}=-\frac{\partial p}{\partial z}+\nu\left(\frac{\partial^2 w}{\partial x^2}+\frac{\partial^2 w}{\partial y^2}+\frac{\partial^2 w}{\partial z^2}\right) \tag{2c}$$

$$\frac{\partial u}{\partial x}+\frac{\partial v}{\partial y}+\frac{\partial w}{\partial z}=0, \tag{2d}$$

where nonlinear terms have been neglected. As underlined by Waleffe and Kim [11], the streak instability associated with equations (2) generates $[vv]$, $[vw]$, $[wv]$ and $[ww]$ Reynolds stresses that inject energy into streamwise rolls (1b) and (1c), while the Reynolds stress components $[uv]$ and $[uw]$ extract energy from the streaky flow (1a). Finally, a Fourier expansion for the perturbation is assumed by considering only one Fourier mode, referenced as $\alpha = 2\pi/L_x$, such as: $\mathbf{u}(x,y,z,t) = \hat{u}(y,z,t)\,e^{i\alpha x} + \hat{u}^{\star}(y,z,t)\,e^{-i\alpha x}$ where superscript $\star$ denotes complex conjugate. The coupled system of equations (1) and (2) constitutes the lowest-order model to maintain a self-sustained cycle and will be referred hereafter as the minimal Restricted Nonlinear (RNL) model. A similar model was employed by Biau and Bottaro [18] and more recently by Pralits et al. [19] to compute nonlinear optimal perturbations in a square duct flow and a Couette flow, respectively. One may also remark that nonlinear bifurcation analysis aiming to take into account mean flow distortion associated with a feedback term that involves the fluctuating Reynolds stress have regained some interest these last years (Mantic-Lugo et al. [20] and Turton et al. [21], for instance).

Fourier expansion is used in the spanwise direction and Chebyshev polynomials are used in the wall-normal direction to discretize the previous system (equations (1) and (2)). A second-order extrapolation and a backward-differentiation scheme are applied to convective and diffusive terms, respectively. To ensure a divergence-free, the Uzawa method is employed for each spanwise Fourier mode (for more details, see [22] and [23]). Finally, the truncated Fourier series are performed with the DFFTPACK library and a pseudospectral technique is used to evaluate explicit terms.

3. Results

In this work, we intend to evaluate the minimal RNL model to describe the periodic orbit and travelling wave solutions located in the bulk of the channel flow recently found by Rawat et al. [14]. For that purpose, similar initial conditions are used. On the one hand, the equation for the streamwise component of the streamwise-averaged flow (1a) is initiated by the laminar Poiseuille solution. On the other hand, the initial condition for equations (1b) and (1c) governing rolls consist in a pair of streamwise uniform counter-rotating vortices of amplitude A_1:

$$U/U_c = 1-(y/h)^2,\ V/U_c = A_1\frac{\partial \psi}{\partial z},\ W/U_c = -A_1\frac{\partial \psi}{\partial y}, \tag{3}$$

with U_c the centreline mean streamwise velocity for the laminar Poiseuille solution and $\psi = (1-(y/h)^2)\sin(\pi y/h)\times \sin(2\pi z/L_z)$. In addition, a sinuous initial condition of amplitude A_2 for the spanwise component of the perturbation (4) is used to trigger the instability of the streaky flow (see also [24]):

$$u=0,\ v=0,\ w/U_c = A_2(1-(y/h)^2)\sin(\alpha x/h). \tag{4}$$

As in Rawat et al. [14], the ratio A_2/A_1 is kept constant to 1/10. A bisection procedure on the initial amplitude A_1 is used to track the edge state solution of the system. Hereafter, $\alpha\ h = 1$ and the Reynolds number $Re = U_c h/\nu$ is varying from 2000 to 5000 (below the critical Reynolds number associated with the onset of an exponential mode). The results shown hereafter are obtained with 100×32 points in the wall-normal, and spanwise directions, respectively. The number of Fourier modes in the spanwise direction is increased up to 64 for the largest spanwise extent that is considered. A constant volume flux is enforced during the simulation.

3.1. Edge tracking

In Figs. 1 and 2, we report for $Re = 3000$, $L_z = 2.2h$ and $L_z = 4h$ the temporal evolution of the kinetic energy for the perturbation $E(t) = \left(\int_{2h\times L_z}\left(\hat{u}^2+\hat{v}^2+\hat{w}^2\right)dy\,dz\right)/(h^2U_c^2)$ and the temporal history of the corresponding streamwise vortices amplitude, defined as $E_{\omega_x}(t) = \left(\int_{2h\times L_z}\omega_x^2\,dy\,dz\right)/(U_c^2)$ where $\omega_x = \partial V/\partial z - \partial W/\partial y$. For the two cases, the initial stage exhibits a similar behaviour. The strength of streamwise vortices are seen to decrease while the kinetic energy of the

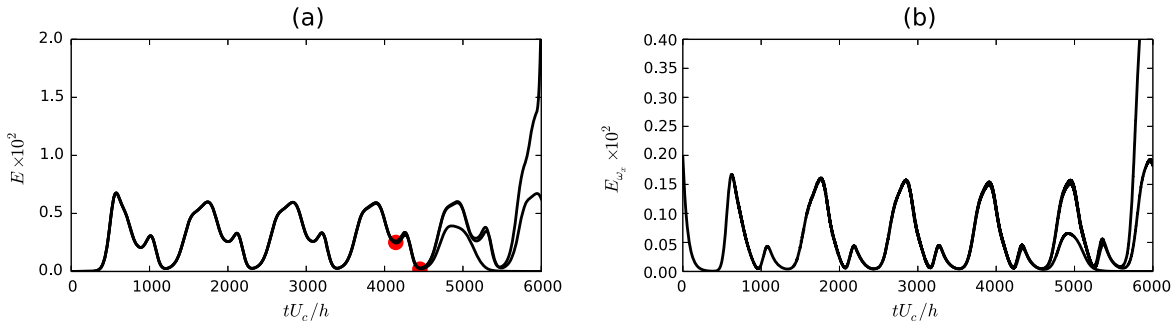

Fig. 1. Minimal RNL system $L_z = 2.2\ h$ and $Re = 3000$. Time evolution of (a) perturbation kinetic energy and (b) square of L^2 norm of the streamwise vorticity for the roll. Three initial amplitudes are considered: $A_0 = 0.00067062839$, 0.000670628401527, and 0.000670628402.

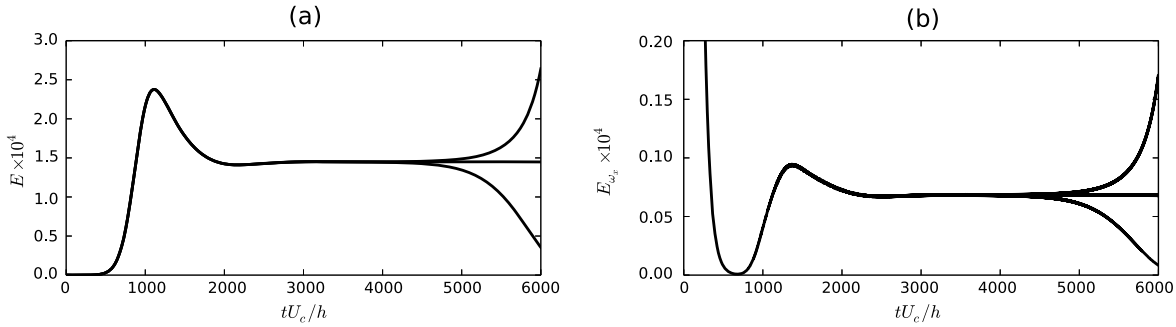

Fig. 2. Minimal RNL system $L_z = 4h$ and $Re = 3000$. Time evolution of (a) perturbation kinetic energy and (b) square of L^2 norm of the streamwise vorticity for the roll. Three initial amplitudes are considered: $A_0 = 0.00059356394$, 0.00059356395, and 0.00059356396.

perturbation associated with the secondary instability of the streak increases. When the perturbation reaches a sufficiently high energy level to regenerate streamwise vortices, we observe an increase in its corresponding amplitude, triggering the onset of the self-sustaining process. In particular, as seen in Figs. 1 and 2, if the bisection is sufficiently refined, solutions of the minimal RNL model are living for a finite time in the boundary of the basin of attraction of the laminar state. Above a critical initial amplitude, the solution is diverging, whereas if the amplitude A_1 remains below its critical value, the solutions converges to the laminar Poiseuille flow. It is interesting to notice that transient roll/streaks dynamics shown in Fig. 2 exhibits strong similarities with direct numerical simulations carried out by Cossu et al. [25].

For all the Reynolds numbers that are considered here, for L_z below $\approx 2.4\ h$, $2.5\ h$, solutions on the edge state converge to a relative periodic orbit. As shown in Fig. 1 for $L_z = 2.2\ h$ and $Re = 3000$, the amplitude of vortices is almost synchronized with the kinetic energy evolution of the perturbation with a slight delay. In addition, the perturbation is seen to have a phase velocity $\approx 0.98\,U_c$ (not shown here for the sake of conciseness). Above $L_z \approx 2.4\ h$, $2.5\ h$, solutions on the edge bifurcate into a travelling wave solution. The streamwise vortices are continuously generated from the feedback exerted by the streak instability on the mean flow dynamics. As a consequence, both kinetic energy of the perturbation and the amplitude of streamwise vortices reach a constant level on the basin of attraction of the laminar flow. The travelling wave solution is seen to propagate with a phase velocity $\approx 0.98\ U_c$.

Travelling wave solutions bifurcating from relative periodic orbits have been recently observed by Rawat et al. [14] using DNS. Invariant solutions given by previous authors are computed for $Re = 2000 - 5000$ and $L_x = 2\pi\ h$ with L_z varying from $2.4\ h$ to $10.5\ h$. Relative periodic orbits and the upper and lower branches of travelling wave solutions are found to collide in a global saddle-node infinite period bifurcation for $L_z \approx 3.55\ h$ and $Re = 2000$. The period of oscillations tends to infinity as the spanwise extent approaches the critical value. In particular, for L_z just below $3.55\ h$, Rawat et al. [14] observed increasingly long quiescent phases separated by relatively quick bursts. While a global bifurcation also occurs in our analysis, at L_z below the one obtained in DNS, final conclusions on similarities between the bifurcation observed by integrating the minimal RNL system and full DNS equations can not be drawn.

3.2. Structure of the relative periodic orbit and travelling wave solution

For times $t = 4143 \times h/U_c$ and $4451 \times h/U_c$ (indicated by full red circles in Fig. 1(a)), the perturbation and mean streamwise velocity components for $L_z = 2.2\ h$ and $Re = 3000$ are shown in Figs. 3 and 4, respectively. The solution is characterized by streamwise vortices occupying the whole spanwise width of the domain and low-speed streaks on both the lower and upper walls. Every half-period of the cycle, low-speed streaks and streamwise vortices are shifted in the

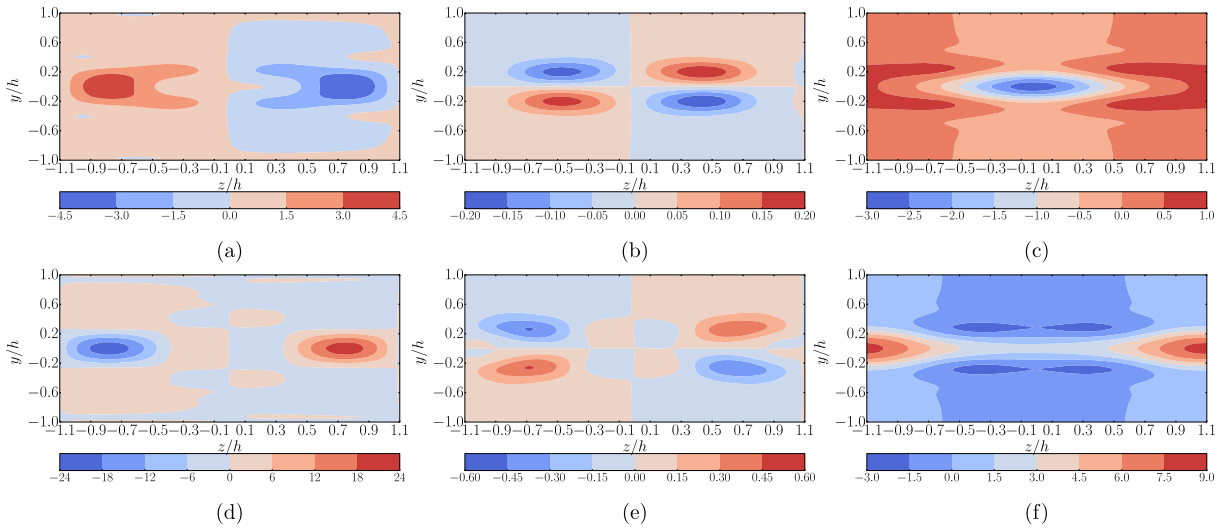

Fig. 3. $Re = 3000$ and $L_z = 2.2\ h$. Real part of the perturbation for $t \times U_c/h = 4143$ and $t \times U_c/h = 4451$ ((a), (b), (c) and (d), (e), (f), respectively). The streamwise, wall normal and spanwise components are represented in (a)(d), (b)(e) and (c)(f), respectively. Contour levels are made dimensionless by U_c and are multiplied by 10^3.

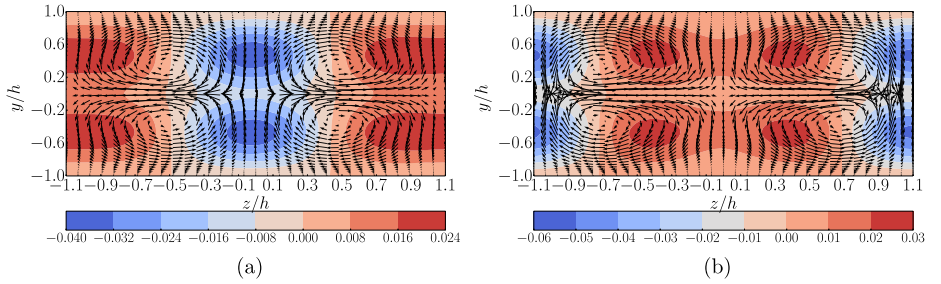

Fig. 4. $Re = 3000$, $L_z = 2.2\ h$. Vector field (W, V) and $U - \overline{U}$ (where $\overline{\bullet}$ denotes the z-averaging operator) at $t \times U_c/h = 4143$ and $t \times U_c/h = 4451$ ((a) and (b), respectively). Contour levels are made dimensionless by U_c.

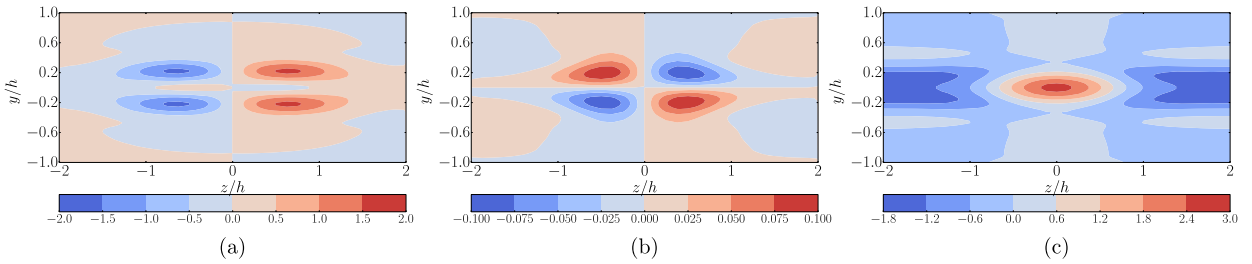

Fig. 5. $Re = 3000$ and $L_z = 4\ h$. The streamwise, wall normal and spanwise components of the perturbation lying on the edge are represented in (a), (b) and (c) respectively. Contour levels are made dimensionless by U_c and are multiplied by 10^3.

spanwise direction. For times $t = 4143 \times h/U_c$ and $4451 \times h/U_c$, as reported in Fig. 3, the perturbation exhibits a sinuous pattern on the flanks of the low-speed streak.

Regarding the travelling wave solution for $L_z = 4\ h$ and $Re = 3000$, Fig. 5 shows that perturbation components are located in the bulk of the flow as for the previous invariant solution. The perturbation rotates counter-clockwise during one period of the travelling wave and exhibits a mid-plane reflection symmetry ($y = 0$). The perturbation acts in a feedback loop to generate time-invariant mean streamwise vortices that in turn create low-speed streaks, due to the lift up effect, close to the channel centre, as shown in Fig. 6. Especially, the solution exhibits a spanwise localization. Furthermore, the perturbation shown in Figs. 5 appears in an anti-symmetric pattern with respect to the plane defined by $z = 0$, which will lead to a sinuous motion of low-speed streaks. When the edge tracking is carried out for higher values of L_z (up to 10 h), the low-speed streak flanked to streamwise vortices are seen to remain almost unchanged. The latter pattern becomes

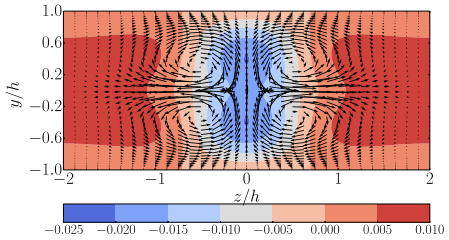

Fig. 6. $Re = 3000$ and $L_z = 4\ h$. Vector field (W, V) and $U - \overline{U}$ (where $\overline{\bullet}$ denotes the z-averaging operator) for the streaky motion lying on the edge state. Contour levels are made dimensionless by U_c.

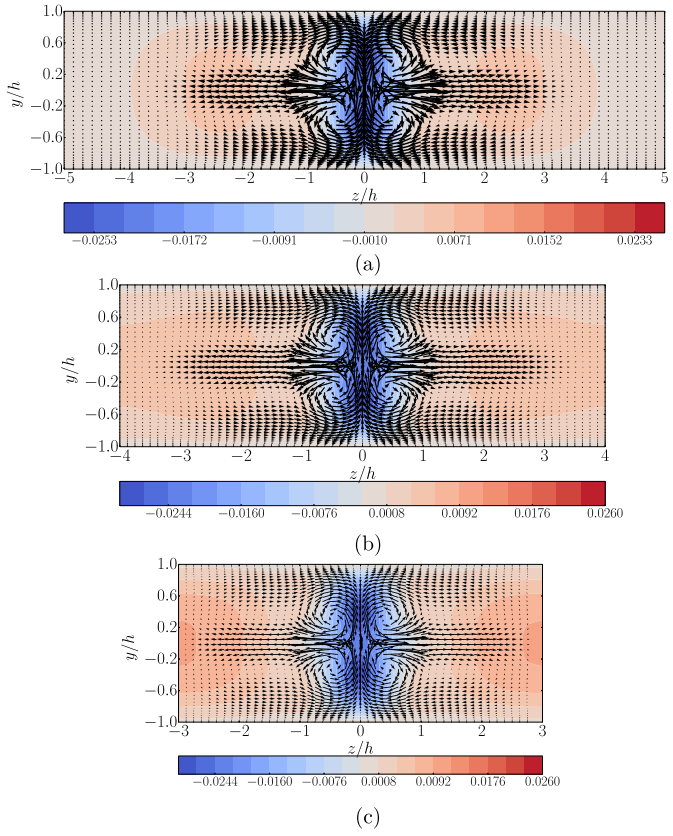

Fig. 7. Invariant solution for $Re = 3000$ and $L_z = 10,\ 8$ and $6\ h$ ((a), (b) and (c), respectively). Vector field (W, V) and $U - \overline{U}$ (where $\overline{\bullet}$ denotes the z-averaging operator) are represented. Contour levels are made dimensionless by U_c.

strongly localized in the spanwise direction and is surrounded by very large regions where the mean streamwise velocity converges toward the laminar Poiseuille flow solution. The results are shown in Fig. 7 where flow cases $L_z = 6,\ 8$ and $10\ h$ are reported for $Re = 3000$. For $L_z < 5\ h$ these localized structures arise naturally by the procedure described above, without the need to use a windowing function. For higher values of the spanwise size, the streak secondary instability is too weak to trigger the self-sustained process. For $5\ h < L_z \leq 10\ h$, the initial condition is built by windowing a pair of streamwise vortices obtained for $L_z/2$.

The flow structures associated with the travelling wave solution derived from the minimal RNL model appear similar to those associated with the lower branch solution computed by a continuation procedure based on the full Navier–Stokes equations [14]. In particular, the spanwise localization of these solutions, their reflectional symmetry about $y = 0$, and their concentration at the centre of the channel are in agreement with the results of Rawat et al. [14]. In addition, previous authors also found that these solutions arise naturally through continuation, which is consistent with our results.

In order to gain some insight into the effects of Reynolds number and spanwise size on these solutions, we introduce the dimensionless quantities $E_s(z) = \left(\int_{2\ h} \left(U - \overline{U}\right)^2 \mathrm{d}y\right) / \left(hU_c^2\right)$ (where $\overline{\bullet}$ denotes the z-average) and $E^z_{\omega_x}(z) =$

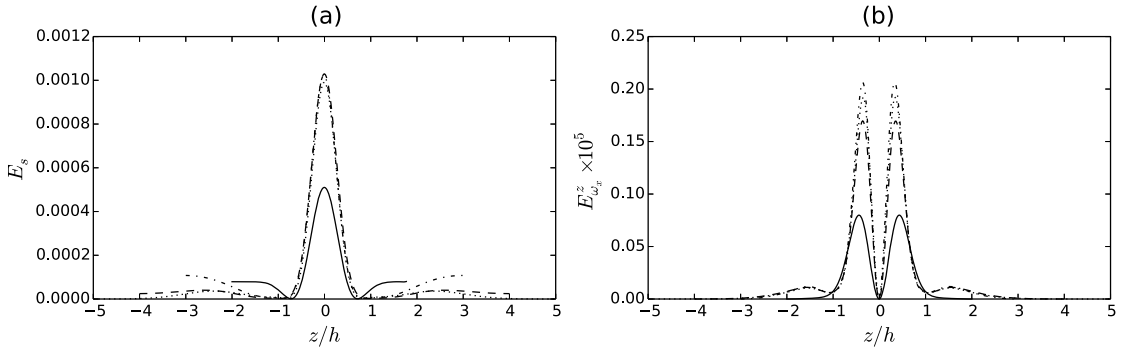

Fig. 8. Travelling wave solution for $Re = 3000$. Distributions of (a) streaks amplitudes and (b) streamwise vortices amplitudes as a function of the spanwise position for $Re = 3000$ and $L_z = 4\ h$ (−), $L_z = 6\ h$ (−·−), $L_z = 8\ h$ (−−) and $L_z = 10\ h$ (···).

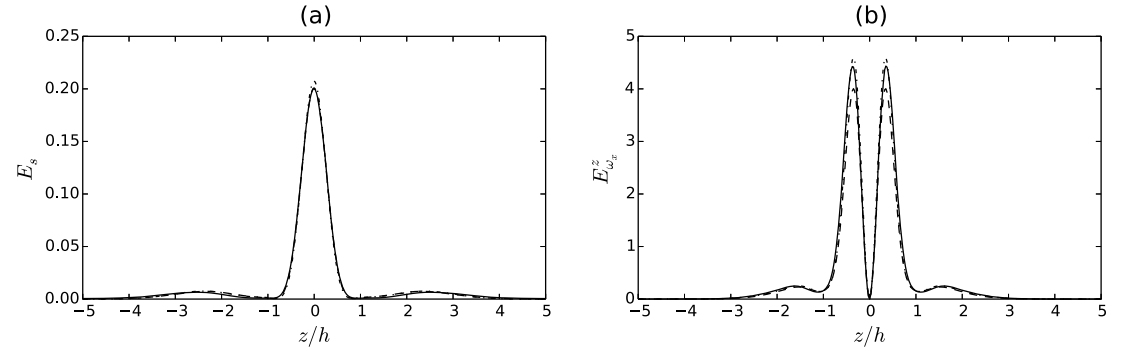

Fig. 9. Travelling wave solution for $L_z = 10\ h$. Distributions of (a) streaks amplitudes and (b) streamwise vortices amplitudes as a function of the spanwise position for $Re = 2000$ (−), $Re = 3000$ (−·−), $Re = 5000$ (−−). E_s and $E^z_{\omega_x}$ are rescaled accounting for their self-similar behaviour.

$\left(\int_{2\ h} \omega_x^2 \mathrm{d}y\right) h/U_c^2$ representing the amplitudes of streaks and streamwise vortices along the spanwise direction, respectively. In Fig. 8, we report distributions of streak amplitudes and streamwise vortices amplitudes for L_z varying from $L_z = 4\ h$ to $L_z = 10\ h$. The figure shows that the solution becomes almost independent of the spanwise extent for L_z wider than $8\ h$.

When the Reynolds number is varying from 2000 to 5000 for $L_z = 10\ h$, the amplitude of streaks is decreasing. In particular, a self-similar behaviour is observed when the latter amplitude is rescaled by a factor $\propto Re^{-a}$ with $a \approx 2$, as shown in Fig. 9(a) in which a perfect collapse is observed for the three Reynolds numbers that are considered. The streamwise vortices also exhibit a self-similar behaviour when their amplitudes are rescaled by a factor $\propto Re^{-1.85a}$ as shown in Fig. 9(b).

As could be expected, the square root of the ratio of streak to streamwise vortices amplitudes is almost proportional to Re ($Re^{0.85}$), which further indicates the importance of the lift-up mechanism in the self-sustaining of these travelling wave solutions. Such self-similar behaviour is also observed for the periodic orbit solution by Rawat et al. [13], where the obtained scaling laws are comparable. In particular, the ratio between streak and rolls found by the latter authors is similar.

4. Discussion

The restricted nonlinear model truncated to a single streamwise mode for the perturbation, referenced as minimal RNL model, has been applied to the study of invariant solutions in a plane channel flow. Flow cases recently investigated by Rawat et al. [14] are considered. The Reynolds number based on the centreline velocity and half-channel height (U_c and h) varies from 2000 to 5000 and the streamwise length is fixed to $2\pi\ h$. The minimal RNL model is seen to reproduce self-sustained roll/streak dynamics that are the key elements of invariant solutions found in wall-bounded flows. Furthermore, by using a bisection procedure on the initial condition given by Rawat et al. [13], the minimal RNL model converges toward either a relative periodic orbit or a travelling wave when the spanwise dimension size is increased from $L_z = 2.2\ h$ to $L_z = 10\ h$. In particular, spanwise-localized travelling wave solutions provided by the minimal RNL system for L_z greater than $\approx 2.4\ h$, $2.5\ h$ are reminiscent of solutions lying on the lower branch computed by Rawat et al. [14] using DNS. They are located in the bulk of the flow and propagate with a phase velocity of $\approx 0.98\ U_c$, as also found in DNS. They also exhibit a self-similar behaviour when increasing the Reynolds number. Although the minimal RNL model fails in accurately predicting the spanwise size of the domain beyond which the period orbit bifurcates into travelling-wave solutions, the invariant solutions display similar structures and roll/streak dynamics.

It may be suggested that the truncation of the RNL model to a single Fourier mode is too severe to determine the exact spanwise extent where travelling waves connect the relative periodic orbit solution. In this context, the analysis of RNL models restricted to a small subset of streamwise Fourier components should be an interesting prospect. Furthermore, the bisection method used in the present study prevents from drawing firm conclusions about whether the global bifurcation found by integrating the minimal RNL system and the one obtained by a Newton–Krylov-based continuation method coupled with a DNS solver are of the same kind [14] (i.e. a global saddle-node–infinite-period bifurcation).

Finally, as underlined recently by Hwang et al. [15], invariant solutions located in the bulk of the flow degenerate into large-scale coherent structures when the effect of small-scale motions are artificially damped. RNL models may thus provide a minimal representation of the organization of large-scale motions in wall-bounded turbulent flows. For that purpose, the investigation of RNL models to approximate invariant solutions associated with the upper branch might be of great interest to further understand recent results provided by Hwang et al. [15].

References

[1] Y. Duguet, C.C.T. Pringle, R.R. Kerswell, Relative periodic orbits in transitional pipe flow, Phys. Fluids 11 (2008) 114102.
[2] R.R. Kerswell, O. Tutty, Recurrence of travelling wave solutions in transitional pipe flow, J. Fluid Mech. 584 (2007) 69–102.
[3] F. Waleffe, Three-dimensional coherent states in plane shear flows, Phys. Rev. Lett. 81 (1998) 4140–4143.
[4] T.M. Schneider, D. Marinc, B. Eckhard, Localized edge states nucleate turbulence in extended plane Couette cells, J. Fluid Mech. 646 (2010) 441–451.
[5] G. Kawara, M. Uhlmann, L. Van Veen, The significance of simple invariant solutions in turbulent flows, Annu. Rev. Fluid Mech. 44 (2012) 203–225.
[6] J. Jimenéz, M. Simens, Low-dimensional dynamics of a turbulent wall flow, J. Fluid Mech. 435 (2001) 81–91.
[7] J.F. Gibson, E. Brand, Spanwise-localized solutions of planar shear flows, J. Fluid Mech. 745 (2014) 25–61.
[8] J. Jimenéz, P. Moin, The minimal flow unit in near-wall turbulence, J. Fluid Mech. 225 (1991) 213–240.
[9] J.M. Hamilton, J. Kim, F. Waleffe, Regeneration mechanisms of near-wall turbulence structures, J. Fluid Mech. 287 (1995) 317–348.
[10] A. Toh, T. Itano, A periodic-like solution in channel flow, J. Fluid Mech. 481 (2003) 67–76.
[11] F. Waleffe, J. Kim, How streamwise rolls and streaks self-sustain in a shear flow, in: R. Panton (Ed.), Computational Mechanics Publications, 1997, pp. 309–332.
[12] T. Duriez, J.-L. Aider, J.E. Wesfreid, Self-sustaining process through streak generation in a flat-plate boundary layer, Phys. Rev. Lett. 103 (2009) 144502.
[13] S. Rawat, C. Cossu, F. Rincon, Relative periodic orbits in plane Poiseuille flow, C. R. Mecanique 342 (2014) 485–489.
[14] S. Rawat, C. Cossu, F. Rincon, Travelling-wave solutions bifurcating from relative periodic orbits in plane Poiseuille flow, C. R. Mecanique 344 (2016) 448–455.
[15] Y. Hwang, A.P. Willis, C. Cossu, Invariant solutions of minimal large-scale structures in turbulent channel flow for Re_τ up to 1000, J. Fluid Mech. 802 (2016) R1.
[16] V.L. Thomas, B.F. Farrell, P.J. Ioannou, D.F. Gayme, A minimal model of self-sustaining turbulence, Phys. Fluids 27 (2015) 105104.
[17] B.F. Farrell, P.J. Ioannou, J. Jiménez, N.C. Constantinou, A. Lozano-Durán, M.-A. Nikolaidis, A statistical state dynamics based study of the structure and mechanism of large-scale motions in plane Poiseuille flow, J. Fluid Mech. 809 (2016) 290–315.
[18] D. Biau, A. Bottaro, An optimal path to transition in a duct, Philos. Trans. R. Soc. A 367 (2009) 529–544.
[19] J.O. Pralits, A. Bottaro, S. Cherubini, Weakly nonlinear optimal perturbations, J. Fluid Mech. 785 (2015) 135–151.
[20] V. Mantic-Lugo, C. Arratia, F. Gallaire, Self-consistent mean flow description of the nonlinear saturation of the vortex shedding in the cylinder wake, Phys. Rev. Lett. 113 (2014) 084501.
[21] S.E. Turton, L.S. Tuckerman, D. Barkley, Prediction of frequencies in thermosolutal convection from mean flows, Phys. Rev. E 91 (2015) 043009.
[22] F. Alizard, Linear stability of optimal streaks in the log-layer of turbulent channel flows, Phys. Fluids 27 (2015) 105103.
[23] R. Peyret, Spectral Methods for Incompressible Viscous Flow, Springer, 2002.
[24] W. Schoppa, F. Hussain, Coherent structure generation in near-wall turbulence, J. Fluid Mech. 453 (2002) 57–108.
[25] C. Cossu, L. Brandt, S. Bagheri, D.S. Henningson, Secondary threshold amplitudes for sinuous streak breakdown, Phys. Fluids 23 (2011) 074103.